

ALL-FIBER THULIUM-DOPED MODE-LOCKED LASERS BASED ON THE NONLINEAR AMPLIFYING LOOP MIRROR

Authors:

M. A. Chernysheva, A.A. Krylov, P.G. Kryukov, N.R. Arutyunyan, A.S. Pozharov, E.D. Obraztsova, E.M. Dianov

DOI: 10.12684/alt.1.89

Corresponding author: M.A. Chernysheva
e-mail: chernysheva_maria@mail.ru

All-Fiber Thulium-Doped Mode-Locked Lasers Based on the Nonlinear Amplifying Loop Mirror

M. A. Chernysheva¹, A.A. Krylov¹, P.G. Kryukov¹, N.R. Arutyunyan², A.S. Pozharov²,
E.D. Obraztsova², E.M. Dianov¹

¹Fiber Optics Research Center of the Russian Academy of Sciences, 38 Vavilov str., Moscow, 119333, Russia

²A.M. Prokhorov General Physics Institute of the Russian Academy of Sciences, 38 Vavilov str., Moscow, 119333, Russia

Abstract

We report on thulium-doped all-fiber lasers based on the nonlinear amplifying loop mirror and mode-locked by both a semiconductor saturable absorber (SESAM) and single-walled carbon nanotubes (SWCNT). An intracavity and external dispersion management was realized with the aid of a passive germanium-silicate fiber. SESAM mode-locked laser generates as short as 230-fs pulses with maximum average output power of 106 mW, corresponding to a 3.7 kW peak power and almost 2 nJ pulse energy. In contrast to SESAM-based laser, the SWCNT mode-locked laser generates 450-fs pulses of mW-level average output power respectively.

Introduction

For the last few years thulium-doped mode-locked fiber lasers operating in a spectral band between 1.8 and 2.1 μm with a high lasing efficiency have been increasingly investigated due to a wide scope of their possible applications, for example in spectroscopy, LIDARs, medicine, and semiconductor micromachining.

Earlier different schemes incorporating SESAMs and SWCNT based saturable absorbers have been reported for thulium-doped mode-locked dispersion-managed fiber lasers [1-4]. Most of them had linear, ring or figure-of-eight cavity geometries. By accurate intracavity dispersion control, the shortest achieved pulse duration was 235 fs with the spectral bandwidth of 22 nm and 20 mW average output power [2].

Recently nonlinear amplifying loop mirror (NALM) has been paid much attention as a fast modulator of laser radiation. NALM benefits originate from breaking the symmetry in the loop with the aid of unequal splitting ratio of the NALM forming fiber coupler and the gain implementation. The nonlinear Kerr effect in a fiber causes an intensity-dependent difference in the optical path lengths for counter-propagating pulses [5]. In addition, polarization control provides appropriate

linear phase delay for pulses propagating in opposite directions [6]. This leads to the intensity dependent loop mirror reflectivity. Thus, due to the intensity dependent reflectivity, NALM incorporation into laser cavity provides efficient self-switching, pedestal suppression and pulse shaping mechanisms. In contrast to CW lasing, GVD management inside the loop substantially promotes NALM operation properties for the short pulse generation by significant CW signal suppression. Due to strictly different evolution of counter-propagating pulses transmitted inside the dispersion-imbalanced loop, there occurs an additional intensity-dependent phase shift [7]. As a result, generated pulses can be switched out the NALM while any CW background signal is reflected by a dispersion-imbalanced loop. Furthermore, the NALM pulse cubing effect results in the efficient background wave suppression and, therefore, pulse interactions reduction [6].

However, there is not clear attitude to what saturable absorber is still the best of all. Here we present a comparison of SESAM and SWCNT mode-locked thulium-doped fiber lasers built with the same elements. Both lasers' setups were formed in a sigma-cavity configuration based on the NALM as an additional fast light modulator.

Experimental setup and results

Both lasers were based on the same elements employing a nonlinear amplifying fiber loop mirror formed by a 20:80 fiber coupler. Here a 0.7 m-long segment of a step-index ($\Delta n = 0.012$) thulium-doped aluminum-silica (0.8 wt% thulium, 3.6 wt% aluminum) glass fiber (TDF) is positioned inside the loop close to the 20% output port of the NALM forming coupler. The TDF dispersion varied monotonically in the 1.2–2.1 μm wavelength range giving $\beta_2 = -76 \text{ ps}^2/\text{km}$ at the wavelength of laser generation near $\sim 1.9 \mu\text{m}$. The active fiber possesses 10 μm core diameter with $\lambda_c \approx 2.2 \mu\text{m}$ cutoff wavelength, and 60 dB/m non-saturated absorption at 1.56 μm . Pump radiation of 1 W maximum power from a CW erbium-ytterbium co-doped fiber laser is coupled into the laser cavity through a

1.56/1.9 μm wavelength division multiplexer (WDM) in a clockwise direction of the NALM.

A short section of low-loss normal dispersion ($\beta_2 = +280 \text{ ps}^2/\text{km}$; $\Delta n \sim 0.11$; $d_{\text{eff}} \sim 3.4 \mu\text{m}$) highly nonlinear ($\gamma = 15 \text{ W}^{-1} \cdot \text{km}^{-1}$) germanium-silica ($\text{GeO}_2/\text{SiO}_2$) glass fiber is spliced into the fiber loop to control the overall net cavity dispersion. Germanium oxide concentration in the fiber core was measured to be 75 mol% [8]. The length of the $\text{GeO}_2/\text{SiO}_2$ fiber was varied during experiments through a cutback method. A squeezing hand-made polarization controller (PC) placed inside the loop provides an efficient lasing wavelength tuning as well as helps to adjust the proper NALM operation regime. An additional commercially available polarization controller inserted into the linear part of the laser cavity ensures stable single-pulse mode-locking operation and helps to improve pulse characteristics.

In order to compensate an excessive pulse chirp, a short section of the same $\text{GeO}_2/\text{SiO}_2$ fiber was implemented outside laser cavity, creating the appropriate external dispersion delay line. A fiber isolator, placed at the output of the laser scheme, prevents laser radiation transmitting back to the laser cavity. Generated laser beam was collimated to ensure a low divergence for further pulse characteristics measurements.

SESAM mode-locked thulium-doped fiber laser

The experimental schematic of the SESAM mode-locked laser containing aforementioned NALM is presented in Fig. 1 [9].

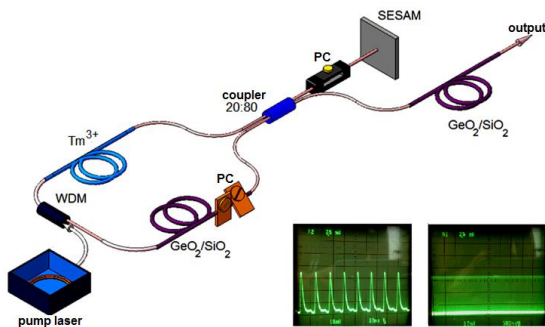


Fig. 1. Layout of SESAM mode-locked thulium-doped fiber laser. Inserts: pulse trains.

A SESAM [10], initiating stable single-pulse mode-locked generation, is attached face-to-face to the 80% coupler output with respect to the counterclockwise propagating beam. Via shortening the $\text{GeO}_2/\text{SiO}_2$ fiber length from 50 to 10 cm, corresponding to the pulse repetition rate ranging from 52 to 58 MHz, the overall net cavity dispersion was varied between -0.054 and -0.11 ps^2 . The laser average output power in this experiment slightly ranged near 9.5 mW at a constant pump power level of 310 mW. An evolution of the pulse duration, spectrum

bandwidth and corresponding time-bandwidth product, measured at the laser output before external compression, is demonstrated in Fig. 2.

In spite of the fact that laser cavity contained fiber segments of opposite GVD signs, soliton-type function [11] fits measured intensity autocorrelation traces more accurate than Gaussian one. Thus, according to the recently developed theory [12], generated pulses could be considered as conservative dispersion-managed (DM) solitons. By varying the intracavity dispersion value, the autocorrelation trace FWHM was ranged from 1.33 ps to 765 fs corresponding to the pulse duration variation between 860 and 490 fs. The pulse spectrum bandwidth oscillated in this case from 6 to 16.6 nm. It should be noticed that spectrum shape did not contain characteristic sharp Kelly-sidebands due to the background dispersive wave suppression in the NALM [6]. However, if the cavity possessed -0.054 ps^2 GVD value (corresponding to 50-cm long intracavity section of $\text{GeO}_2/\text{SiO}_2$ fiber), the estimated time-bandwidth product was much higher than characteristic value inherent to solitons (0.315) and amounted to ~ 1 , resulting in the slightly chirped pulse generation. Corresponding pulse-length was measured to be $\Delta\tau_p = 725 \text{ fs}$ at a spectrum bandwidth of $\Delta\lambda = 16.6 \text{ nm}$. An excess chirp value indicates that pulses could be further compressed in a properly adjusted external dispersion delay line.

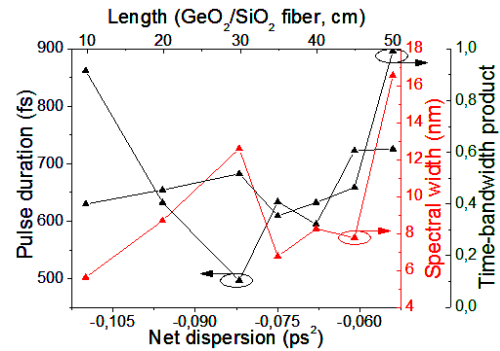


Fig. 2. Evolution of SESAM mode-locked laser pulse characteristics by varying the intracavity dispersion

Owing to the external dispersion management at the laser output by means of the 31-cm-long $\text{GeO}_2/\text{SiO}_2$ fiber, the shortest pulses of slightly less than 230 fs with a spectrum FWHM of as large as 26.4 nm were achieved in the case of intracavity and external GVD values of -0.054 ps^2 and -0.031 ps^2 respectively. After compression the time-bandwidth product was more than 2 times reduced, giving its value of $\Delta\nu \cdot \Delta\tau \sim 0.48$. The output spectrum and autocorrelation trace of pulse intensity are shown in Fig. 3 (green plots).

Via pump power increase from 310 mW up to 1 W, the laser has been still operating without perturbations in a single-pulse regime generating

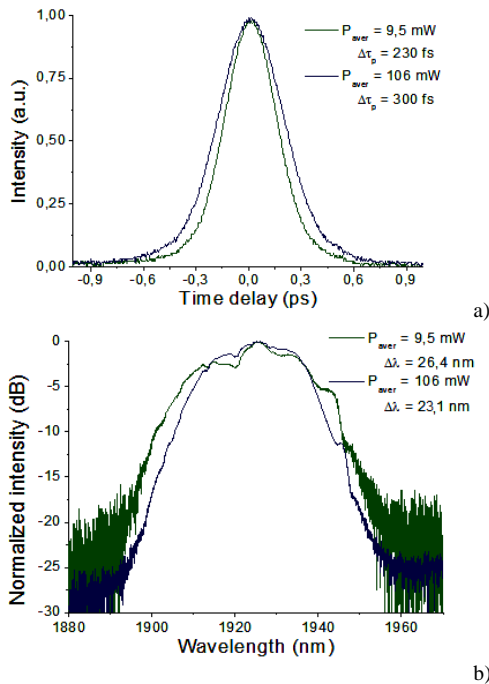


Fig. 3. SESAM mode-locked laser output pulse characteristics: a) autocorrelation traces; b) spectra at the different average

near 300 fs soliton-type pulses, which characteristics are shown in Fig. 3 (blue plots). At the same time, spectrum shape was not changed substantially in the course of pump power increase, giving its -3-dB-level bandwidth close to ~23.1 nm.

It should be noticed, that measured spectrum peak intensity value at 1925 nm increased linearly with almost the same factor as pump power did (Fig. 4a). In addition, the maximum average output power was also increasing strictly linearly without any

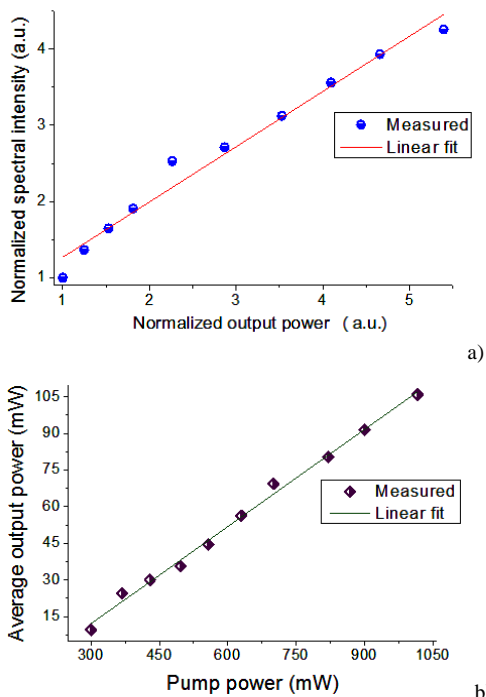


Fig. 4. a) Normalized spectral intensity dependence on average output power; b) Laser efficiency

saturation dynamics, as it is demonstrated in Fig. 4(b). Therefore, it is possible to make a quite obvious assumption that pump power can be further increased for higher laser powers to be achieved. Unfortunately, we were limited by the maximum pump power of 1 W corresponding to the TDF-laser output average power of 106 mW and ~2 nJ pulse energy. Taking into account 300 fs pulse-length and figures given above, the estimated laser peak power reached as much as 3.7 kW.

SWCNT mode-locked thulium-doped fiber laser

The laser setup is presented in Fig. 5 [13]. Laser cavity is formed by linear and aforementioned nonlinear fiber loop mirrors. The linear mirror (FLM) provided reflectivity of 88% at 1.9 μm. A SWCNT based saturable absorber was formed with the help of two angle-polished ferrules of optical APC-connectors (SAINT-module) and was positioned at the same point in the cavity as SESAM was.

The SWCNTs were synthesized by the arc discharge method in the helium atmosphere with the means of Ni – Y₂O₃ catalyst in the C:Ni:Y₂O₃ 2:1:1 mixture filling a graphite anode. It is well known that the SWCNTs produced by arc discharge method possess an optical absorption band shifted to IR-wavelength range comparing to the absorption bands of nanotubes synthesized using other methods [14]. Manufacturing and characteristics of stable suspensions of individual SWCNTs in 1 wt% aqueous solution of carboxymethylcellulose (CMC) is described in details in [15].

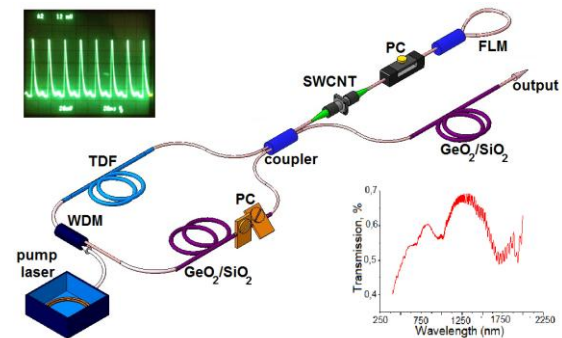


Fig. 5. Schematic sketch of the thulium-doped SWCNT mode-locked fiber laser. Inserts: pulse trains (at the top), CMC film transmission spectrum (at the bottom).

Cellulose was chosen as a key element to form high optical quality polymer films because it is both an efficient surfactant and a matrix material. Due to this fact, only two elements (CMC and SWCNTs) are needed to arrange the suspension in order to create high optical quality films. Cellulose, in turn, is rather high-flexible polymer, which makes possible to form thin films of a thickness down to 4 or 6 μm. The most stable mode-locking operation occurs by using two films simultaneously in one

saturable absorber module providing the total transmission value of 57.6% at 1.9 μm (see the insert in Fig. 5). SWCNT diameter was estimated by Raman spectroscopic analysis to be about 1.4 nm.

While $\text{GeO}_2/\text{SiO}_2$ fiber length inside the NALM was cut back from 80 to 15 cm, the overall net cavity dispersion varied from -0.044 to -0.131 ps^2 . The external dispersion value was preserved at the same level of -0.031 ps^2 as in the case of SESAM mode-locked thulium-doped fiber laser setup. The pulse repetition period ranged from 25 to 22 ns corresponding to the pulse repetition frequency oscillation between 40 and 45.5 MHz.

Figure 6 presents an evolution of the pulse intensity autocorrelation trace full-width at half-maximum (FWHM), spectrum bandwidth and time-bandwidth product through the intracavity GVD variation. Pump power during these experiments was also adjusted at a constant level of 310 mW as in the previous experiments. However, TDF-laser average output power slightly decreased and oscillated around 6.3 mW.

As the dispersion map was created in the laser cavity, the autocorrelation trace kept near soliton-like envelope for large values of anomalous GVD but, in turn, was fitted quite accurately by Gaussian curve for near zero anomalous GVD values [13]. The soliton-like pulse-length varied between 450 and 620 fs as it is seen in Fig. 6. For example, in the case of -0.124 ps^2 intracavity GVD value, 520 fs soliton pulses ($\Delta\nu \cdot \Delta\tau = 0.32$) with a -3-dB spectral bandwidth of 7.33 nm were generated.

The shortest pulse-length of slightly less than 450 fs was measured at the intracavity dispersion value of -0.093 ps^2 . Corresponding spectrum bandwidth reached in this case 15.8 nm. Laser spectrum and autocorrelation trace of pulse intensity are presented in Fig. 7 (blue plots).

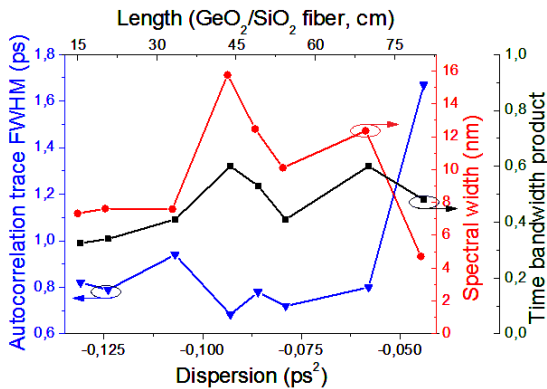


Fig. 6: Evolution of SWCNT mode-locked laser output characteristics through the intracavity dispersion variation

A pump power increase up to 560 mW results in the preserving a single-pulse operation regime, giving 18 mW average power and $\sim 0.4 \text{ nJ}$ pulse energy

respectively. The pulse duration was estimated to be 640 fs with a spectrum FWHM of 7.6 nm, which corresponds to $\sim 625 \text{ W}$ peak power (Fig. 7, blue plots). It should be noticed that further pump power increase was limited by the damage threshold of CMC polymer films.

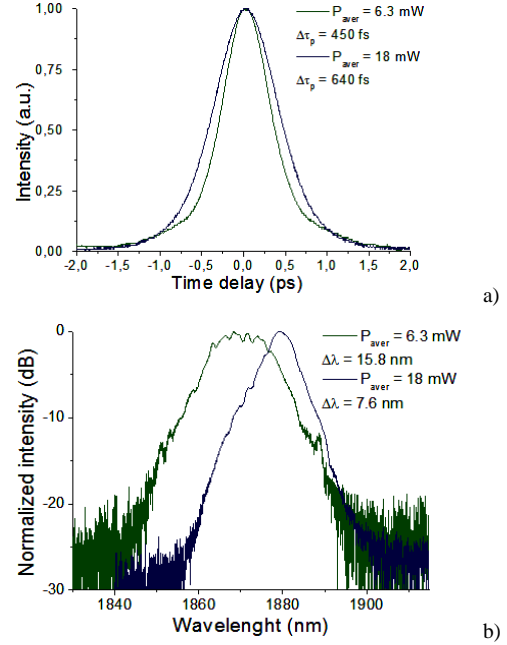


Fig. 7. SWCNT mode-locked laser pulse characteristics: a) autocorrelation traces of pulse intensity; b) spectra at different average powers.

Temporal transmission of NALM for pulses with a power $P(t)$ could be estimated as [16]:

$$T(t) = 1 - 2\rho \cdot (1 - \rho) \cdot \{1 + \cos(1 - \rho - G\rho) \cdot \gamma \cdot P(t) \cdot L\} \quad (1)$$

Here ρ is the bar port transmission of the coupler, G – active fiber total gain, and L is the loop length. In addition, if the next condition is fulfilled:

$$(G - 1) \cdot \gamma \cdot P_{peak} \cdot L = 2k\pi \quad (2)$$

then the central part of the pulse is transmitted without significant losses, while pulse wings are weakened [16]. Such loss dependence on light intensity is similar to the amplitude modulation induced by fast saturable absorber providing high-quality pulse formation mechanism.

Actually, it is difficult to calculate the real transmission of the NALM for given laser setups, because pulses entering the NALM possess characteristics, which we are not aware of. However, it may be quite interesting to estimate NALM operation peculiarities using measured output pulse parameters together with given laser ones. As it is seen in Fig. 8, the NALM transmission dependence on a pulse peak power shows several maxima corresponding to strongly different pulse powers. This fact is in good agreement with NALM operation theory [17]. It is

worth noting, that these maxima correspond to either the shortest pulses or the longest ones.

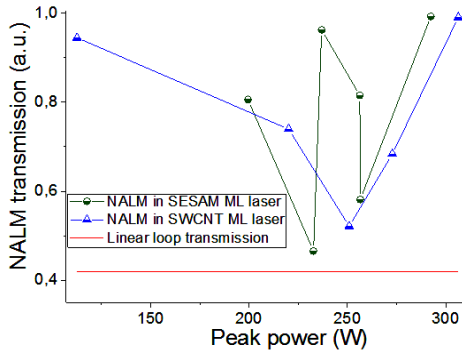


Fig. 8: Evolution of NALM transmission by varying the pulse peak power

Figure 9 provides an understanding of how the total GVD inside the NALM influences on its transmission value. It is undoubtedly seen in Fig. 9 that in the case of near zero dispersion inside the loop, NALM transmission reaches its maximum regardless of the input pulse parameters such as pulse length or peak power.

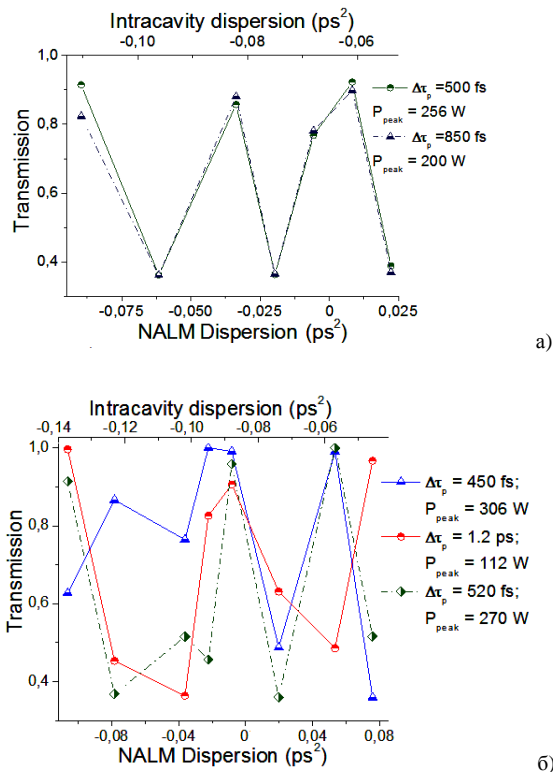


Fig. 9: Evolution of NALM transmission in the SESAM mode-locked laser (a) and SWCNT mode-locked laser (b) by varying the intracavity and NALM dispersion.

Thus, we may suggest that for generation of shortest pulses with widest spectrum in the NALM based mode-locked laser, the total dispersion inside a loop has to be close to zero. It is quite different from the well-known stretched-pulse lasers, whose total intracavity dispersion must be near zero for shortest pulse generation [18].

Conclusion

In conclusion, we have demonstrated two layouts of all-fiber thulium-doped lasers based on the NALM and mode-locked by either SESAM or SWCNT based saturable absorber. In general, both lasers demonstrate quite resembling generation peculiarities based on properties of the NALM acting as an additional fast modulator. Thus, by an appropriate intracavity and external dispersion control, laser pulse-length was strongly shortened while the pulse spectrum quality was improved by Kelly side-bands suppression. In addition, we have observed that for shortest pulse generation the total dispersion inside the NALM has to be close to zero. Lasers generate as short as 230-fs pulses through the SESAM implementation and 450-fs pulses using SWCNT CMC films as a saturable absorber. To the best of our knowledge, we have observed the shortest pulses ever generated by the SESAM and SWCNT mode-locked thulium-doped fiber lasers.

Acknowledgements

The authors would like to acknowledge I.A. Bufetov, M.A. Mel'koumov and V.M. Mashinsky from the Fiber Optics Research Center of RAS for fiber providing, as well as O.G. Okhotnikov from the Tampere University of Technology for SESAM production. We are also thankful to A.K. Senatorov from the Fiber Optics Research Center of RAS and B.L. Davydov from the Institute of Radio engineering and Electronics of RAS for technical support.

References

- [1] R. Gumenyuk, I. Vartiainen, H. Tuovinen and O.G. Okhotnikov (2010), Dissipative dispersion-managed soliton 2 μm thulium/holmium fiber laser, *Opt. Lett.* 36(5), 609-11
- [2] Q. Wang, T. Chen and K. Chen (2010), Mode-locked ultrafast thulium fiber laser with all-fiber dispersion management, in *Proc. of OSA/CLEO/QELS Conference, CFK7*
- [3] M.A.Solodyankin, E. D. Obraztsova, A.S. Lobach and A.I. Chernov (2008), Mode-locked 1.93 μm thulium fiber laser with a carbon nanotube absorber, *Opt. Lett.* 33, 1336-38
- [4] K.Kieu and W.Wise (2009), Soliton thulium-doped fiber laser with carbon nanotube saturable absorber, *IEEE Photon Tech. Lett.* 21(3), 128-30
- [5] M. E. Fermann, F. Haberl, M. Hofer and H. Hochreiter (1990), Nonlinear amplifying loop mirror, *Opt. Lett.* 15(13), 752-54
- [6] K. Smith, N. J. Doran and P. G. J. Wigley (1990), Pulse shaping, compression, and pedestal

suppression employing a nonlinear-optical loop mirror, *Opt. Lett.* 15, 1294-96

[7] W. S. Wong, S. Namiki, M. Margalit, H. A. Haus and E. P. Ippen (1997), Self-switching of optical pulses in dispersion-imbalanced nonlinear loop mirrors, *Opt. Lett.* 22, 1150-52

[8] E. M. Dianov, and V. M. Mashinsky (2005) Germania-Based Core Optical Fibers, *Journal of LIGHTWAVE TECHNOLOGY*, 23 (11), 3500-08

[9] M. A. Chernysheva, A. A. Krylov, P. G. Kryukov and E. M. Dianov (2012), Nonlinear Amplifying Loop Mirror Based Mode-Locked Thulium Doped Fiber Laser, *IEEE Photon. Tech. Lett.* 24(14), 1254-56

[10] S. Kivittstö, T. Hakulinen, M. Guina, and O.G. Okhotnikov (2007), Tunable Raman soliton source using mode-locked Tm-Ho fiber laser, *IEEE Photon. Tech. Lett.* 19, 934-36

[11] J.-C. M. Diels, J. J. Fontaine, I. C. McMichael, and F. Simoni (1985) Control and measurement of ultrashort pulse shapes (in amplitude and phase) with femtosecond accuracy, *Appl. Opt.* 24(9), 1270-85

[12] B.G. Bale, S. Boscolo, and S.K. Turitsyn (2009) Dissipative dispersion-managed solitons in mode-locked lasers *Opt. Lett.* 34(21) 3286-88

[13] M. A. Chernysheva, A. A. Krylov, P. G. Kryukov, N. R. Arutyunyan, A. S. Pozharov, E. D. Obraztsova and E. M. Dianov (2012) Thulium-doped mode-locked all-fiber laser based on NALM and carbon nanotube saturable absorber in *Proc. ECOC (OSA)*, Tu.4.F.4.

[14] E. D. Obraztsova, J.-M. Bonard, V. L. Kuznetsov, V. I. Zaikovskii, S. M. Pimenov, A. S. Pozharov, S. V. Terekhov, V. I. Konov, A. N. Obraztsov and A. P. Volkov (1999) Structural measurements for single-wall carbon nanotubes by Raman scattering technique, *Nanostruct. Mater.* 12 567-72

[15] A. I. Chernov, E. D. Obraztsova and A. S. Lobach (2007) Optical properties of polymer films with embedded single-wall carbon nanotubes, *Phys. Stat. sol (b)* 224(11), 4231-35

[16] G.P. Agrawal (2001) *Applications of nonlinear fiber optics*, Academic Press, San Diego

[17] I. N. Duling III, C.-J. Chen, P. K. A. Wai and C. R. Menyuk (1994) Operation of a nonlinear loop mirror in a laser cavity, *IEEE J. Quant. Electron.* 30(1) 194-99

[18] L. E. Nelson, D. J. Jones, K. Tamura, H. A. Haus, and E. P. Ippen (1997) Ultrashort-pulse fiber ring lasers, *Appl. Phys. (b)* 65(2), 277-94